Anti-CD63 antibodies suppress IgE-dependent allergic reactions in vitro and in vivo

Stefan Kraft, Tony Fleming, James M. Billingsley, Shih-Yao Lin, Marie-Hélène Jouvin, Peter Storz, and Jean-Pierre Kinet

Department of Pathology, Beth Israel Deaconess Medical Center, Harvard Medical School, Boston, MA 02215

High-affinity IgE receptor (FcεRI) cross-linking on mast cells (MCs) induces secretion of preformed allergy mediators (degranulation) and synthesis of lipid mediators and cytokines. Degranulation produces many symptoms of immediate-type allergic reactions and is modulated by adhesion to surfaces coated with specific extracellular matrix (ECM) proteins. The signals involved in this modulation are mostly unknown and their contribution to allergic reactions in vivo is unclear. Here we report the generation of monoclonal antibodies that potently suppress FcεRI-induced degranulation, but not leukotriene synthesis. We identified the antibody target as the tetraspanin CD63. Tetraspanins are membrane molecules that form multimolecular complexes with a broad array of molecules including ECM protein-binding β integrins. We found that anti-CD63 inhibits MC adhesion to fibronectin and vitronectin. Furthermore, anti-CD63 inhibits FcεRI-mediated degranulation in cells adherent to those ECM proteins but not in nonadherent cells. Thus the inhibition of degranulation by anti-CD63 correlates with its effect on adhesion. In support of a mechanistic linkage between the two types of inhibition, anti-CD63 had no effect on FcεRI-induced global tyrosine phosphorylation and calcium mobilization but impaired the Gab2–PI3K pathway that is known to be essential for both degranulation and adhesion. Finally, we showed that these antibodies inhibited FcεRI-mediated allergic reactions in vivo. These properties raise the possibility that anti-CD63 could be used as therapeutic agents in MC-dependent diseases.

CORRESPONDENCE
Jean-Pierre Kinet:
jkinet@bidmc.harvard.edu

Abbreviations used: DNP-HSA, DNP-human serum albumin; ECM, extracellular matrix; FcεRI, high affinity IgE receptor; ITAM, immunoreceptor tyrosine-based activation motif; ITIM, immunoreceptor tyrosine-based inhibition motif; LTC4, leukotriene C4; MC, mast cell; PCA, passive cutaneous anaphylaxis; PI3K, phosphatidylinositol-3 kinase; PI4K, phosphatidylinositol-4 kinase; PKCδ, protein kinase C-δ; PTK, protein–tyrosine kinase; RBL, rat basophilic leukemia.

Mast cells (MCs) are important effectors of immediate-type allergic responses and play a role in host defense and autoimmune diseases (1–4). Activated MCs adhere to extracellular matrix (ECM) proteins such as fibronectin, vitronectin, and laminin (5, 6) that bind to integrin adhesion molecules. MCs express various integrins (e.g., VLA-4 α4β1, VLA-5 α5β1, the vitronectin receptor αvβ3). Adhesion is enhanced by activation of cell surface receptors such as c-Kit or FcεRI (7, 8). In turn, MC adhesion to ECM proteins amplifies FcεRI-induced secretion (9, 10). Antibodies recognizing the integrins α4β1, α5β1, and αvβ3 suppress MC degranulation. Used in combination, they suppress anaphylaxis (11).

The signaling cascade triggered upon FcεRI cross-linking is induced by the activation of protein–tyrosine kinases (PTK) of the Src family, such as Lyn, which phosphorylates the intracellular immunoreceptor tyrosine-based activation motifs (ITAMs) present in the β and γ chains of FcεRI (12). Signaling molecules bearing SH2 domains then bind these phosphorylated ITAMs, leading to the formation of associated multiprotein complexes. The pathway controlled by Lyn leads to the formation of a signaling complex organized around the LAT adaptor involving Vav, SLP-76, Grb2-Sos-Ras, PLCγ, and phosphatidylinositol-3 kinase (PI3K). An essential molecule in the formation of these complexes is the PTK Syk, which phosphorylates and activates multiple molecules downstream. This pathway induces calcium (Ca^{2+}) mobilization and putatively regulates degranulation via the Ca^{2+}-dependent PKCβ. Downstream of Syk activation, the MAP kinase pathway leads to phospholipase A2 activation, an initial step in the production of arachidonic acid metabolites such as leukotriene C4 (LTC4) and prostaglandin D2 (13–15). A second signaling pathway leading to degranulation has been identified (16). It is initiated by the Fyn PTK. Fyn activation promotes the formation of a signaling complex organized around the Gab2 adaptor (17),

The Journal of Experimental Medicine

Downloaded from www.jem.org on February 7, 2005

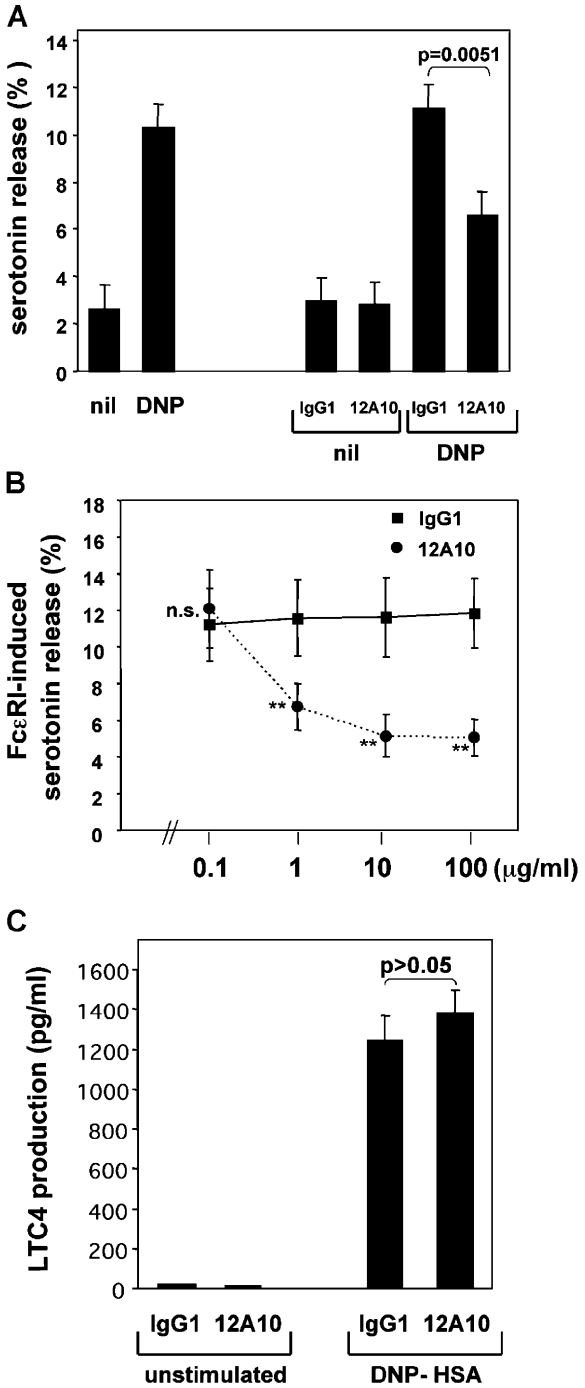

Figure 1. mAb 12A10 suppresses FcεRI-induced serotonin release, but does not inhibit LTC4 production. (A) Serotonin release from RBL-2H3 cells loaded with 0.2 μg/ml anti-DNP IgE and stimulated with DNP-HSA (DNP; 50 ng/ml) to induce FcεRI cross-linking or with vehicle (nil) for 30 min. Results are expressed as percentage of total serotonin uptake (mean ± SEM of five experiments in duplicate). The two columns on the left are for cells without mAb preincubation. The four columns on the right are for cells preincubated with IgG1 control or 12A10 mAb (2 μg/ml) for 30 min before FcεRI triggering. (B) Dose response of inhibition of FcεRI-induced serotonin release by 12A10 or IgG1 control. Cells were triggered as in A. Results are expressed as mean ± SEM of four experiments with duplicate samples. ** P = 0.0117. (C) LTC4 production induced by FcεRI aggregation (50 ng/ml DNP-HSA for 20 min) in RBL-2H3 cells preincubated with 10 μg/ml of IgG1 or 12A10 (mean ± SEM of two experiments in triplicate; P = 0.7532).

which contains SHP-2 and a PI3K. PI3K activation in this complex provides a Ca^{2+}-independent signal for degranulation by subsequent activation of PDK-1 and the Ca^{2+}-independent protein kinase C-δ (PKCδ).

Several inhibitory receptors suppress FcεRI-induced MC functions. They include the MC function–associated molecule MAFA, gp49BI, FcγRIIB, and the paired immunoglobulin-like receptor PIR-B (18). All possess an intracellular inhibitory signaling motif, the immunoreceptor tyrosine-based inhibition motif ITIM. Upon activation, ITIM phosphorylation leads to the recruitment and activation of tyrosine phosphatases such as SHP-1, or inositol phosphatases such as SHIP, which suppress signaling in its early stages.

Inhibition of FcεRI-dependent MC degranulation by antibodies directed against tetraspanins has been reported, but the mechanism is not known. Our laboratory has described a mAb against CD81 that suppresses MC degranulation (19). Another mAb directed against the rat AD1 antigen was also reported to inhibit FcεRI-induced degranulation moderately (20). It was shown later that this mAb recognizes the CD63 molecule that belongs to the tetraspanin family (21). No additional data clarifying its role in MCs have been published since then. Tetraspanins (or transmembrane-4 superfamily proteins) comprise a large family of proteins (22, 23) that are not known to have extracellular ligands. They form membrane complexes by lateral interactions with other tetraspanins and other molecules such as β integrins. Tetraspanins may regulate integrin functions by interfering with integrin signaling, localization, or trafficking (23, 24). CD63 interacts with the α3, α4, and α6 chains of β1 integrins (25, 26) and modulates adhesion (27). Given our current knowledge about tetraspanins in cell migration and adhesion, these molecules may play a similar role in MC biology. However, their role in MCs has not been studied extensively.

In this study, we have generated mAbs against rat basophilic leukemia (RBL)-2H3 cells. These mAbs potently suppress FcεRI-induced MC degranulation in vitro and allergic reactions in vivo. We have identified the antibody target as the CD63 tetraspanin. Anti-CD63 mAbs are able to suppress both adhesion to vitronectin and fibronectin and degranulation of MC grown on these substrates. Furthermore, we show that anti-CD63 specifically suppresses degranulation and Gab2-dependent signaling such as PKCδ activation, in adherent cells, but not in nonadherent cells.

RESULTS

Generation and characterization of mAbs inhibiting FcεRI-dependent MC degranulation

To identify membrane proteins capable of modulating FcεRI-dependent effector functions, we produced mAbs against RBL-2H3 cells, a well-characterized MC model. The mAbs 7A6 and 12A10 were identified as potent sup-

Downloaded from www.jem.org on February 7, 2005

pressors of FcεRI-induced degranulation, as determined by serotonin release in adherent RBL-2H3 cells. Fig. 1 A shows that preincubation with the 12A10 mAb at 2 μg/ml had a significant suppressive effect on degranulation ($P = 0.0051$). At this concentration, FcεRI-induced degranulation in 12A10-treated cells was inhibited by 47% compared with IgG1-treated cells. Dose response experiments showed that a 12A10 concentration of 1 μg/ml already resulted in significant suppression of FcεRI-induced serotonin release, with near-maximal inhibition occurring at 10 μg/ml (Fig. 1 B). Similar data were obtained using the 7A6 mAb (unpublished data). We then investigated whether other MC functions such as production of arachidonic acid metabolites were affected by these mAbs. In contrast to serotonin, which is stored in preformed granules and released upon MC activation, arachidonic acid metabolites are synthesized de novo and secreted upon MC activation. In addition, some late signals required for both events are different, with degranulation being mainly dependent on FcεRI-induced PKC activation and arachidonic acid metabolites being mainly dependent on MAP kinase-induced phospholipase A2 activation (13, 15, 16, 28). Fig. 1 C shows that LTC4 production after FcεRI cross-linking for 20 min was not significantly affected by 12A10 preincubation. These data show that these mAbs selectively suppress serotonin release, without affecting synthesis of lipid mediators.

Identification of the antibody target as CD63

We next identified the molecule(s) recognized by these inhibitory mAbs. Immunoprecipitation with one of the mAbs followed by immunoblotting with either one showed that both mAbs recognized the same 50–60-kD molecule(s) (Fig. 2 A and unpublished data). Cross-competition experiments using excess of one unlabeled mAb to block binding of the other FITC-labeled mAb followed by flow cytometric analysis demonstrated that both 7A6 and 12A10 mAbs bound to the same or adjacent epitopes (unpublished data). The target molecule was found to be heavily *N*-glycosylated (>50%), as treatment with *N*-glycanase yielded a sharp band at 25 kD in immunoblots (unpublished data). The antibodies recognize the protein only in its nonreduced form. As CD63 possesses properties similar to these, we tested whether these mAbs recognize CD63. We took advantage of an Ab directed against the AD1 antigen, which recognizes CD63 (20, 21). Immunoprecipitation and blotting of RBL cell lysates with anti-AD1 identified a 50–60-kD protein similar to that identified by 12A10 (Fig. 2 A, left). Immunoprecipitation with 12A10 and blotting with anti-AD1, and the converse, appeared to detect the same protein as that identified by anti-AD1 (Fig. 2 A). These experiments suggested that the molecule recognized by 12A10 and 7A6 was rat CD63. To confirm this, we cloned the cDNA for rat CD63 from RBL-2H3 cDNA and expressed it in the human cell line U937. Note that 12A10 and 7A6 do not recognize human or mouse CD63. Cells stably transfected with a FLAG-tagged form of CD63 were tested for reactivity with 12A10 and 7A6. Immunoprecipitation with 12A10 yielded a band of the expected size in transfected cells, but not in untransfected cells (Fig. 2 B, top). Similar results were obtained by immunoprecipitating with anti-FLAG and blotting with

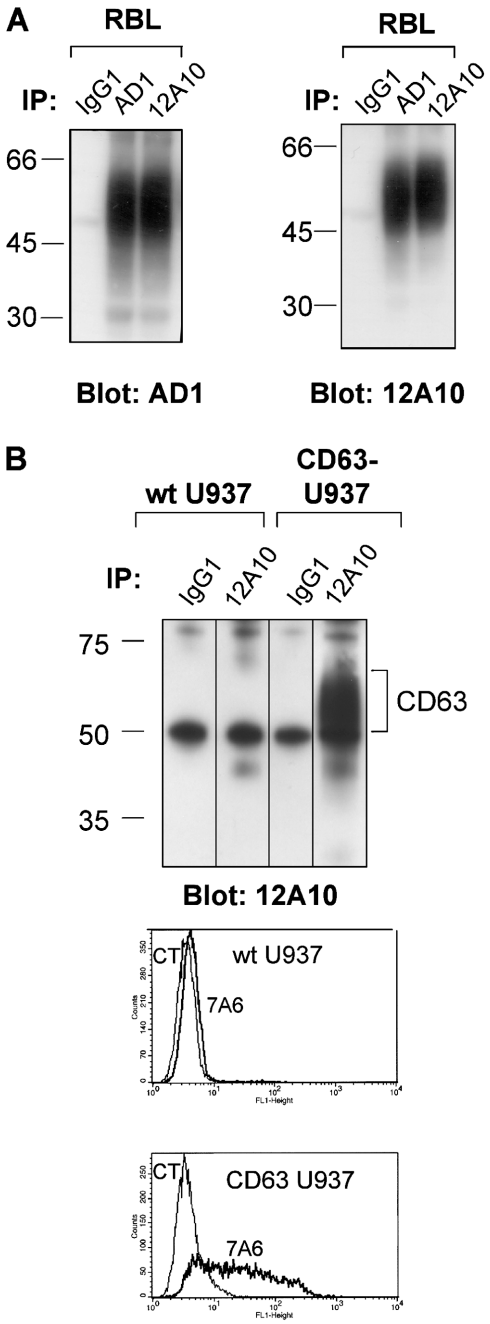

Figure 2. The inhibitory 7A6 and 12A10 mAbs recognize rat CD63. (A) RBL cell lysates were immunoprecipitated with 12A10, an anti-rat CD63 antibody (AD1), or isotype control (IgG1), and immunoblotted with either AD1 or 12A10 mAb. (B, top) Lysates from WT U937 cells and from U937 cells stably transfected with rat CD63 were immunoprecipitated with 12A10 or isotype control and immunoblotted with 12A10 mAb. (B, bottom) WT U937 cells and U937 cells stably transfected with rat CD63 were incubated with 7A6 or control isotype followed by FITC–anti-mouse and analyzed by flow cytometry.

Downloaded from www.jem.org on February 7, 2005

12A10 (unpublished data). Staining with 7A6 and analysis by flow cytometry showed that 7A6, but not an isotype control, reacted with the cell surface of CD63-transfected cells, and not with untransfected cells (Fig. 2 B, bottom). Thus, we concluded that the antigen recognized by 7A6 and 12A10 is the tetraspanin CD63.

Anti-CD63 inhibits MC adhesion to fibronectin and vitronectin and potently suppresses degranulation of adherent MCs

We next investigated the relationship between CD63 and MC adhesion and degranulation. CD63 interacts with the α3, α4, and α6 chains of β1 integrins and is involved in β1 integrin function (25–27). Adhesion of MCs to surfaces coated with the β1 integrin substrate fibronectin enhances FcεRI aggregation induced degranulation (9, 10). In addition, RBL-2H3 cells adhere to fibronectin, vitronectin and fibrinogen, and antibodies against the fibronectin- and vitronectin-binding integrins α4β1, α5β1, and αvβ3 inhibit degranulation and anaphylaxis (11). To test a possible link between degranulation and adhesion in the effect of anti-CD63 on MC, we assessed whether the inhibitory effect of anti-CD63 on degranulation observed with adherent cells was detected in cells stimulated in suspension. Cells were loaded with anti-DNP IgE and [^{3}H]serotonin. They were next either detached and maintained in suspension, or left adherent. Both samples were preincubated with anti-CD63 or isotype control (4 μg/ml). Cells were then triggered with 50 ng/ml DNP-HSA for 20 min. Fig. 3 shows that anti-CD63 pretreatment induced a 46% inhibition of FcεRI-induced serotonin release compared with the isotype control in adherent cells ($P < 0.05$). In contrast, anti-CD63 had no significant effect on cells in suspension. To ensure that the lower release observed with adherent cells incubated with anti-CD63 was not due to the detachment of cells by anti-CD63, we verified that [^{3}H]serotonin incorporation was identical in cells treated with isotype control and cells treated with anti-CD63 (unpublished data). We also verified that the lack of effect of anti-CD63 on cells in suspension was not due to a loss of the epitope due to trypsinization by performing anti-CD63 staining and flow cytometric analysis of cells detached with EDTA or with trypsin. The mean fluorescent intensity of CD63 expression was 87.00 (arbitrary units) for cells detached with 0.02% EDTA alone and 110.51 for cells detached with 0.05% trypsin and EDTA (mean of $n = 3$). Note that RBL cells, in contrast to immature MC, adhere spontaneously to many surfaces, probably as a result of the activating mutation of c-Kit they harbor.

These results suggested that the inhibitory effect of anti-CD63 on MC could be mediated via an effect on MC adhesion to fibronectin and vitronectin present in FCS. To specifically assess the effect of anti-CD63 on integrin-mediated adhesion, we analyzed RBL adhesion to various ECM proteins. Fibronectin and vitronectin enhance MC degranulation, whereas fibrinogen provides a strong attachment factor

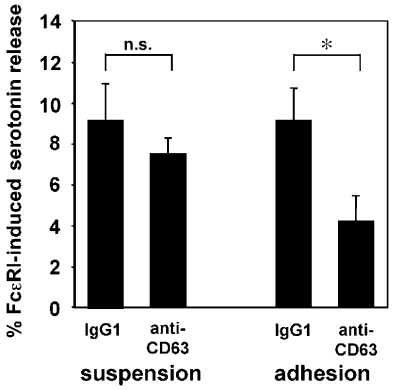

Figure 3. Anti-CD63 suppresses degranulation in adherent cells, but not in cells in suspension. The capacity of anti-CD63 (12A10 mAb) to inhibit FcεRI-induced degranulation was compared in RBL cells that were stimulated either in suspension or adherent (mean ± SEM of six experiments with duplicate samples). * $P = 0.0051$. Cells were loaded with [^{3}H]serotonin and anti-DNP–IgE and triggered, or not, with 50 ng/ml DNP-HSA for 20 min.

for MCs, but has not been shown to enhance mast cell degranulation (11). Cells were incubated with anti-CD63 or IgG1 control (10 μg/ml) and then plated in dishes that had been coated with one of these ECM proteins or left uncoated, and blocked with BSA. After a 30-min incubation at 37°C, nonadherent cells were removed by washing and cell adherence was determined. Fig. 4 A shows that anti-CD63 strongly inhibited adhesion of RBL to fibronectin and vitronectin in a dose-dependent manner compared with the isotype control. Anti-CD63–mediated inhibition of adhesion to fibronectin was of the same order of magnitude as inhibition by the corresponding anti-integrin Abs anti-α5 and anti-β1 used together. However, anti-CD63–mediated inhibition of adhesion to vitronectin was stronger than inhibition by the corresponding anti-integrin anti-β3, possibly because of the expression of other vitronectin binding integrins besides αvβ3 integrin in MC. In contrast to the inhibition of adhesion to fibronectin and vitronectin, adhesion to fibrinogen was not affected by anti-CD63.

These experiments showed that anti-CD63 was capable of inhibiting adhesion to fibronectin and vitronectin, both of which are known to enhance degranulation. In contrast, anti-CD63 had no effect on adhesion to fibrinogen, which is not known to affect degranulation. This suggested that anti-CD63 targets a mechanism that is responsible for modulation of degranulation by adhesion to these ECM proteins. If this was correct, then anti-CD63 should inhibit degranulation of cells adhering to fibronectin and vitronectin, but not fibrinogen. To test this, we compared the capacity of anti-CD63 to inhibit degranulation in cells adhering to these ECM proteins. Fig. 4 B shows a strong suppressive effect of anti-CD63 on degranulation when cells were attached to fibronectin and vitronectin, although the effect was nonsignificant when cells were attached to fibrinogen or plated in uncoated wells. Note that we did not observe the enhancement of degranulation under adherent conditions published previously

Downloaded from www.jem.org on February 7, 2005

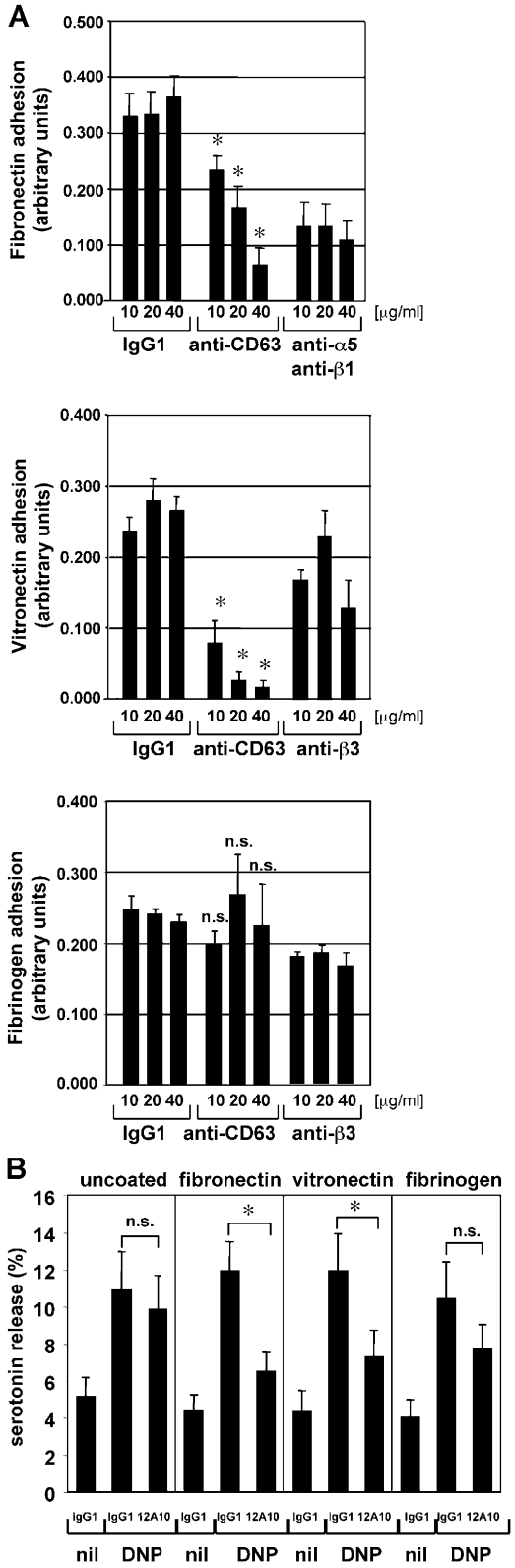

Figure 4. Anti-CD63 potently suppresses both degranulation and adhesion on fibronectin and vitronectin, but not fibrinogen. (A) The capacity of anti-CD63 to inhibit adhesion to fibronectin, vitronectin, and fibrinogen was compared in RBL cells preincubated with control IgG1 or anti-CD63 (12A10) and plated for 30 min at 37°C on 96-well plates coated with fibronectin, vitronectin, or fibrinogen. Adhesion was quantified by crystal violet uptake measured by spectrophotometry at 570 nm in cell lysates and is expressed in arbitrary units after subtracting the value for adhesion to uncoated wells. Results are expressed as mean ± SEM of seven samples (fibronectin) or six samples (vitronectin and fibrinogen). *$P < 0.05$ of anti-CD63–treated cells versus IgG1-treated cells. Antibodies directed against the α5 and β1 chain of β1 integrins or against β3 integrins were used as positive controls. (B) The capacity of anti-CD63 (12A10 mAb at 10 μg/ml) to inhibit FcεRI-induced serotonin release was compared in anti-DNP IgE-loaded RBL cells that were grown for 16 h in the absence of FCS on uncoated wells or surfaces coated with fibronectin, vitronectin, or fibrinogen. All wells were blocked with 2% BSA solution before adding cells. Shown are mean percentage of serotonin release ± SEM from 12 samples (fibronectin), 10 samples (vitronectin and fibrinogen), and 8 samples (uncoated). * $P < 0.05$.

(9, 10; Figs. 3 and 4 B). This may be due in part to technical reasons. The RBL cells we used adhere spontaneously to tissue culture plates and polypropylene tubes, and constant agitation had to be used to minimize adhesion. Together these results show that anti-CD63 inhibits both adhesion to fibronectin and vitronectin, and degranulation of MC grown on these substrates while leaving the degranulation of non-adherent MC intact.

Anti-CD63 leaves FcεRI-induced global tyrosine phosphorylation and Ca^{2+} mobilization intact

The next question was to determine the mechanism of the dual inhibition of adhesion and degranulation. Therefore, we systematically tested the effect of anti-CD63 on various steps of the FcεRI signaling pathways. We first assessed the effect of anti-CD63 on the first event observed after FcεRI aggregation, which is activation of PTKs and subsequent tyrosine phosphorylation of numerous substrates. Global tyrosine phosphorylation was measured by blotting of total cell lysates prepared after 1 to 20 min of triggering with antigen (50 ng/ml DNP-HSA) in adherent cells pretreated with 12A10 (10 μg/ml) or vehicle. Fig. 5 A shows that FcεRI aggregation-induced tyrosine phosphorylation was unaffected by anti-CD63. Therefore, it is unlikely that anti-CD63 inhibits activation of PTKs, such as Lyn, which is responsible for phosphorylation of the FcεRI β and γ chains and for activation of numerous molecules such as Syk, LAT, or SLP-76. However, this does not rule out that anti-CD63 could inhibit directly or indirectly the tyrosine phosphorylation of discrete signaling molecules downstream. To confirm that Lyn activity was not affected by anti-CD63, we tested the effect of anti-CD63 on Ca^{2+} mobilization, a signal dependent on Lyn (29). FcεRI-induced Ca^{2+} mobilization was measured with fura-2 in adherent cells. There was no significant difference between the average Ca^{2+} traces of cells pretreated with IgG1 and those of cells pretreated with the anti-CD63 mAb 12A10 (Fig. 5 B). We verified in parallel (same conditions) that anti-CD63 preincubation did suppress degranulation (unpublished data). Note that the absence of effect of the anti-CD63 on tyrosine phosphorylation and Ca^{2+} mobilization essentially rules out the possibility that the inhi-

Downloaded from www.jem.org on February 7, 2005

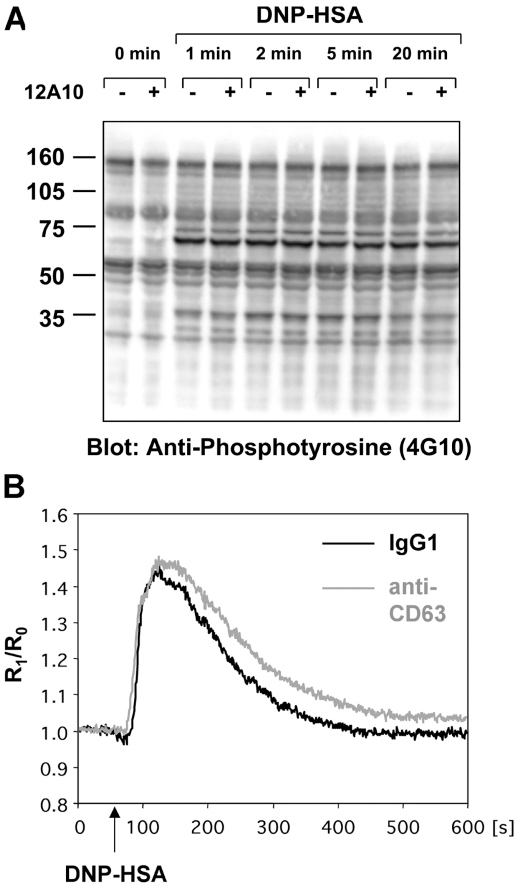

Figure 5. Anti-CD63 leaves FcεRI-induced global tyrosine phosphorylation and Ca^{2+} mobilization intact. (A) Whole cell lysates of unstimulated (0 min) and FcεRI-triggered (DNP-HSA) RBL-2H3 cells preincubated with 12A10 (+) or vehicle (−) were blotted with the anti-phosphotyrosine antibody 4G10. Cells were stimulated under adherent conditions. The data are representative of four experiments. (B) RBL-2H3 cell were preincubated with 10 μg/ml of 12A10 or control IgG1 and loaded with fura 2-AM. Ca^{2+} mobilization induced by FcεRI triggering (50 ng/ml DNP-HSA) was measured in a spectrofluorometer and expressed as the ratio of emission with excitation at 340 and 380 nm. Shown are average traces from 11 for IgG1 (black lines) and 10 experiments for anti-CD63 (gray lines). Ratios (R) at each time point after addition of DNP-HSA were normalized to the baseline ratio during the first 60 s of recording (R_0).

bition could be due to cocrosslinking with the inhibitory receptor FcγRIIB (30).

Because anti-CD63 did not affect the synthesis of arachidonic acid metabolites (Fig. 1 C), which is induced by MAP kinase-triggered PLA2 activation (13–15), we hypothesized that the MAP kinase pathway was insensitive to anti-CD63. We used phosphorylation of the p42 and p44 MAP kinase (Erk1 and Erk2) as a read-out. Adherent cells were pretreated with 10 μg/ml anti-CD63 and triggered with 50 ng/ml DNP-HSA for 2 and 10 min. Indeed, FcεRI-induced phosphorylation of p42 and p44 MAP kinase was readily detectable but not affected by anti-CD63 (unpublished data).

Based on these results we hypothesized that anti-CD63 might specifically affect Ca^{2+}-independent signals that are not part of the pathway controlled by Lyn.

Anti-CD63 inhibits Gab2-dependent signal transduction, which results in diminished activity of the Ca^{2+}-independent PKCδ isoform in adherent cells

Degranulation is controlled by a newly described pathway that involves a complex organized by the Gab2 adaptor (16, 17). This complex is known to contain PI3K, which is responsible for generating PtdIns-3,4,5-trisP (PIP3), a membrane lipid that binds pleckstrin homology (PH) domains and targets PH domain–containing proteins to the plasma membrane. Comparable Gab2 signaling complexes exist also in β integrin signaling (31). We hypothesized that the inhibitory effect of anti-CD63 might be due to the targeting of these Gab2 complexes. To test this hypothesis, we analyzed the effect of anti-CD63 on Gab2 activation. Upon FcεRI aggregation, Gab2 is tyrosine phosphorylated and recruited to the plasma membrane (16, 17, 32). We analyzed tyrosine phosphorylation of Gab2 on anti-Gab2 immunoprecipitates by antiphosphotyrosine blot (Fig. 6 A, representative of three similar experiments). We observed an inhibition of FcεRI-induced tyrosine phosphorylation by anti-CD63 (10 μg/ml) at early time points. This is confirmed by the disappearance with anti-CD63 pretreatment of the mobility shift observed after FcεRI triggering on the anti-Gab2 blot (Fig. 6 A, right). This mobility shift has been attributed to the phosphorylation of Gab2. We then predicted that FcεRI aggregation-induced translocation of Gab2 would be inhibited by anti-CD63, whereas that of Syk, which is dependent on the Lyn-mediated tyrosine phosphorylation of FcεRIγ would not. Indeed, Gab2 translocation to the plasma membrane induced by FcεRI aggregation was decreased after anti-CD63 pretreatment (10 μg/ml), although Syk translocation was unaffected (Fig. 6 B representative of three similar experiments). The lack of effect of anti-CD63 on Syk translocation confirms our findings that the Lyn pathway is unaffected by anti-CD63 (Fig. 5).

To confirm that anti-CD63 targets Gab2 signaling, we analyzed signaling molecules downstream of Gab2. PI3-kinase–dependent kinase-1 (PDK-1) is an effector of Gab2 and participates in the activation of the protein kinase Akt/PKB, another component of FcεRI signaling (33). Akt is activated by phosphorylation by PDK-1 after recruitment to the plasma membrane via the binding of its PH domain to PIP3 (34, 35). We assessed the effect of anti-CD63 on membrane translocation and phosphorylation of Akt after FcεRI aggregation. As expected, anti-CD63 (10 μg/ml) suppressed membrane translocation of Akt (Fig. 6 B representative of three similar experiments). A strong inhibition of Akt serine phosphorylation, which is commonly used as a marker for PIP3 production, was detected as well (Fig. 6 C representative of three similar experiments). Anti-CD63 even inhibited Akt phosphorylation in resting adherent cells. This is in line with our observation that Gab2 translocation, which is also dependent on PH domain–mediated binding to membrane phospholipids (36), was suppressed below basal levels by anti-CD63 (Fig. 6 B). Akt and PI3K play a prominent role in fibronectin- and vitronectin-induced β integrin sig-

Downloaded from www.jem.org on February 7, 2005

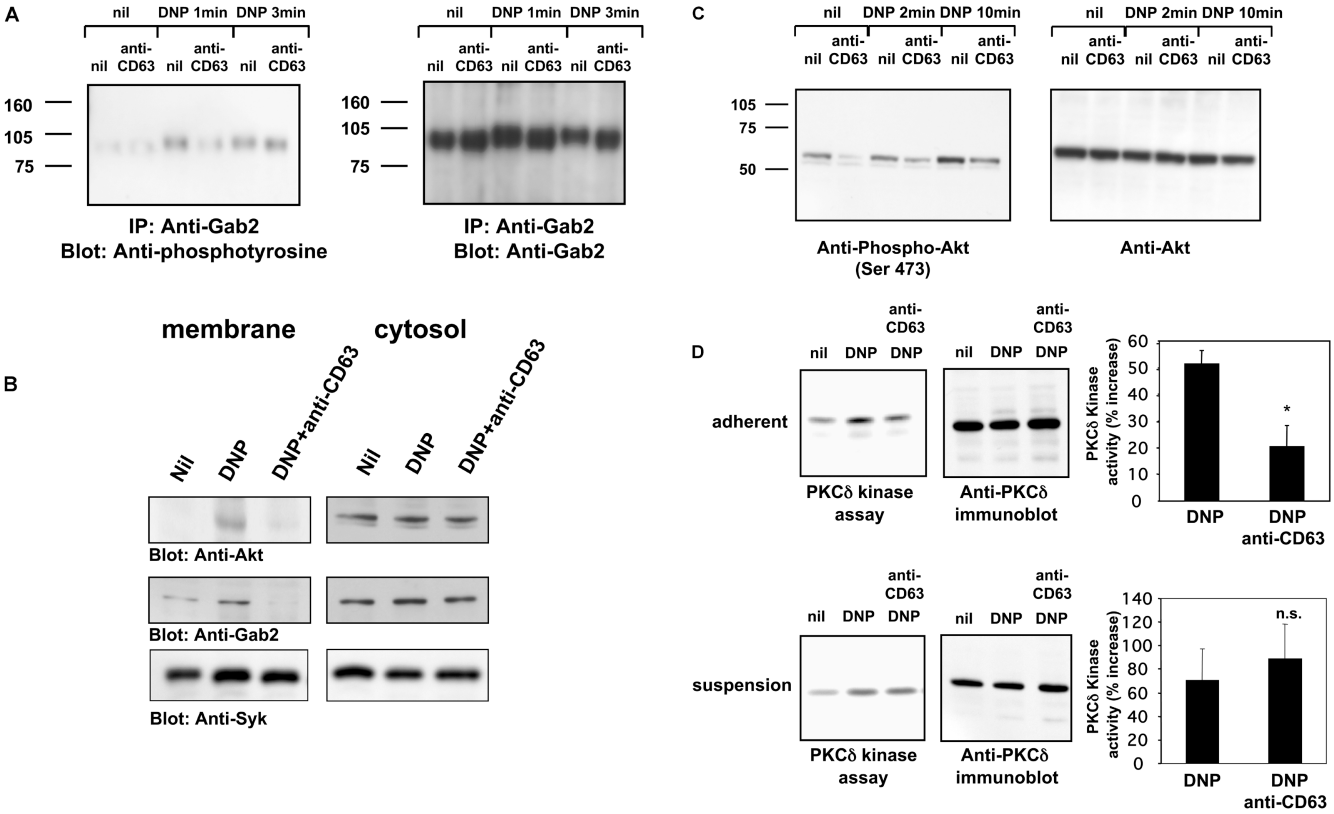

Figure 6. Anti-CD63 inhibits Gab2-dependent signal transduction, which results in diminished activity of the Ca^{2+}-independent PKCδ isoform in adherent cells. (A) Adherent RBL-2H3 cells were preincubated with 12A10 or left untreated. They were then either left unstimulated (nil) or stimulated by FcεRI cross-linking (DNP). Cells were then lysed and Gab2 was immunoprecipitated. Immunoprecipitates were blotted with anti-phosphotyrosine mAb 4G10 (left) or with anti-Gab2 (right). These data are representative of three experiments. (B) Adherent RBL-2H3 cells were stimulated as described for A for 2 min. After lysis, plasma membrane fractions were separated from cytosolic fractions and subjected to immunoblotting with anti-Akt, anti-Gab2, and anti-Syk antibodies. These data are representative of three experiments. (C) Adherent RBL-2H3 cells were stimulated as described for A. Whole cell lysates were immunoblotted with anti-phospho–Akt (left) and anti-Akt (right) to confirm that equal amounts were loaded. These data are representative of three experiments. (D) RBL-2H3 cells, either adherent (top) or in suspension (bottom) were preincubated with 12A10, and either left unstimulated (nil) or stimulated by FcεRI cross-linking for 3 min (DNP). Cells were then lysed and PKCδ was immunoprecipitated. Immunoprecipitates were subjected to in vitro kinase assay using MBP as substrate (left). The immunoprecipitates were blotted with anti-PKCδ to confirm that equal amounts of PKCδ were immunoprecipitated (middle). A densitometric analysis of the MBP band in in vitro kinase assays was performed (right) and the results are expressed as mean ± SEM of percent increase after FcεRI aggregation compared with baseline activity in six (adherent) or three (suspension) experiments. *P = 0.0277 of anti-CD63–treated cells versus vehicle-treated cells.

naling and function as well (37–40). Thus, this suppression of basal Akt activation suggests that anti-CD63 inhibits β integrin signals. A second function of PDK-1 is to activate PKCδ, a novel, Ca^{2+}-independent PKC isoform that is critical for degranulation in RBL cells (28), and which participates in the β integrin signaling pathways (41). To investigate the effect of anti-CD63 on FcεRI-induced activity of PKCδ, we stimulated adherent RBL cells by FcεRI cross-linking and assessed PKC activity by in vitro kinase assay using myelin basic protein (MBP) as a substrate. PKCδ kinase activity was induced and this activation was suppressed by preincubation with 12A10 in adherent cells (Fig. 6 D, top, representative of six similar experiments). However, when the experiment was performed on cells in suspension, PKCδ was activated by FcεRI effectively, but this activation was not inhibited by anti-CD63 (Fig. 6 D, bottom, representative of three similar experiments). As an additional control we chose to analyze another novel PKC isoform, PKCε, which is activated upon FcεRI triggering, but does not seem to play a role in degranulation. As expected, PKCε kinase activity was induced by FcεRI but was not affected by anti-CD63 pretreatment (unpublished data). The lack of sensitivity of PKCε, a negative regulator of PLA2 (42, 43), is in agreement with the insensitivity of arachidonic acid synthesis induction to anti-CD63 (Fig. 1 C).

All together, these results demonstrate that the anti-CD63 targets a Ca^{2+}-independent signaling pathway characterized by Gab2 and PKCδ, which controls degranulation and is also essential in signaling by β integrins.

Anti-CD63 suppresses passive cutaneous anaphylaxis in vivo

Suppression of both MC adhesion and MC degranulation could represent a method of treating MC-mediated diseases. For this reason, we next assessed the efficacy of anti-CD63

Downloaded from www.jem.org on February 7, 2005

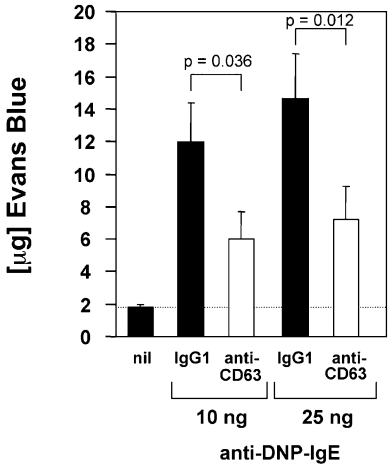

Figure 7. Anti-CD63 suppresses passive cutaneous anaphylaxis reactions in rats. Rats were sensitized intradermally with 10 or 25 ng anti-DNP IgE along with 50 μg 12A10 or control IgG1 in duplicate sites. 24 h later PCA was induced by i.v. injection of DNP-HSA along with Evan's Blue. The skin sites were excised, Evan's Blue was extracted, and quantified by absorbance at 610 nm. The results are expressed as mean ± SEM of μg Evan's Blue (four duplicate experiments).

in suppressing allergic reactions involving normal tissue–resident MCs in vivo. In a passive cutaneous anaphylaxis (PCA) model, antigen-specific IgE is injected into the back skin of rats. An immediate-type allergic reaction is induced by injection of antigen and Evan's Blue dye. MC activation through FcεRI in PCA results in the release of several vasoactive substances, which increases vascular permeability. This property can be quantified by local accumulation of the Evan's Blue dye leaving the vessels in the area of previous IgE injection. These results are expressed as micrograms of Evan's Blue dye extracted from tissue biopsies. As shown in Fig. 7, coinjection of anti-CD63 mAb significantly inhibited IgE-dependent PCA reactions. Importantly, the extent of inhibition of IgE-mediated anaphylaxis with 58.6% (10 ng anti-DNP IgE) and 57.3% suppression (25 ng anti-DNP IgE) was comparable to the highest levels achieved in vitro. These data demonstrate that anti-CD63 can suppress allergic reactions in vivo.

DISCUSSION

We have generated mAbs that were selected based on their capacity to inhibit FcεRI-induced MC degranulation in vitro (Fig. 1, A and B). Two of these mAbs recognize CD63, a tetraspanin that can associate with β integrins (22, 23, 25, 26, 44), the cell surface proteins responsible for adhesion to ECM proteins (Fig. 2). These mAbs inhibit degranulation of adherent MC but not of nonadherent MC (Fig. 3). In addition, these mAbs inhibit MC adhesion to fibronectin and vitronectin, the ECM proteins that amplify MC degranulation (9–11) but not to fibrinogen, which has no known effect on degranulation (Fig. 4). Furthermore anti-CD63 inhibits degranulation of MC adhering to fibronectin and vitronectin, but not of MC adhering to fibrinogen (Fig. 4). In terms of the molecular mechanism of this inhibition, we show that anti-CD63 inhibits the FcεRI-mediated PI3K–Gab2–PKCδ pathway that leads to degranulation (Fig. 6), whereas the Lyn–Ca^{2+} mobilization pathway is unaffected (Fig. 5). Anti-CD63 is also inhibitory when tested in an animal model of allergic reactions, suggesting that it has potential therapeutic value (Fig. 7).

Adhesion has been shown to modulate FcεRI-induced degranulation in several studies (9–11). However the molecular events responsible for the crosstalk between adhesion and degranulation are not well understood. Please note that for the sake of simplicity we use the term adhesion for a variety of complex processes that include static adhesion (i.e., the binding of integrins to substrates and cell attachment) and dynamic adhesion (e.g., integrin-mediated spreading of cells to ECM surfaces, adhesion strengthening upon shear flow). It is likely that tetraspanins play a role in dynamic adhesion. For example, CD81 is involved in α4β1 and α5β1 integrin–mediated adhesion strengthening in monocytes and B cells under shear flow (45). In fact the supportive effect of adhesion for MC degranulation has been attributed to cell spreading (9).

A role for the focal adhesion kinase FAK in adhesion-enhanced degranulation has also been proposed (46, 47). However, FcεRI function is normal in FAK-deficient MC (48). Therefore, it is unlikely that FAK plays a major role in amplification of degranulation by adhesion.

Another pathway involved in integrin-mediated adhesion that could potentially modulate degranulation involves the adaptor Fyn-binding protein (FYB/SLAP–130/ADAP). In MCs, FYB enhances adhesion to fibronectin and mediator release after FcεRI aggregation (49). However, FYB amplifies degranulation in nonadherent as well as adherent cells (49). In preliminary experiments we assessed FcεRI-mediated tyrosine phosphorylation of FYB and found that it was not affected by anti-CD63 (unpublished data). Therefore, the mechanism targeted by anti-CD63 is probably different from the one involving FYB.

Our results show that anti-CD63 inhibits the Gab2–PI3K–PKCδ signaling pathway that is common to degranulation and adhesion. These data shed new light on the molecular connections between FcεRI-mediated degranulation and adhesion. We propose that membrane complexes containing CD63 control MC adhesion and regulate FcεRI-induced degranulation via a shared signaling pathway. Fig. 8 shows a schematic representation of this pathway. Besides Lyn, FcεRI aggregation induces the activation of Fyn in BMMC. In RBL cells, Fyn expression is very low, thus another PTK could play the role of Fyn (16, 32). This event, along with Syk activation, promotes the formation of a complex that involves PI3K and the adaptor Gab2. Gab2 is necessary for PI3K activation, and, in turn, the PI3K product $PI3,4,5P_3$ (PIP3) promotes the recruitment of Gab2 to the plasma membrane via its PH domain. PI3K products also promote the recruitment and activation of PDK-1 and Akt, which is then activated by phosphorylation by PDK-1. PDK-1 also activates PKCδ (16), which results in degranulation. Signaling by β integrins involves the generation of

Downloaded from www.jem.org on February 7, 2005

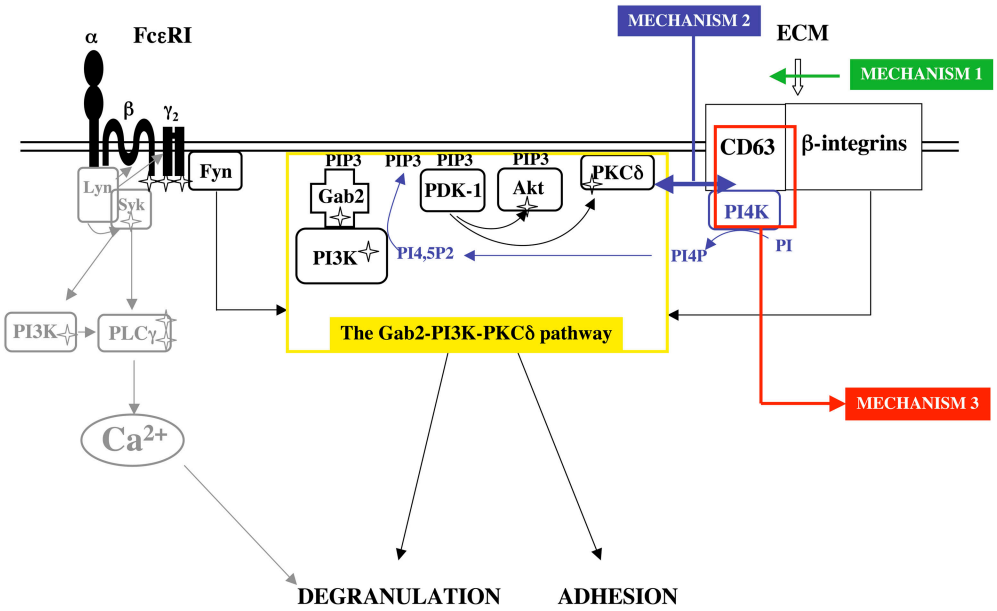

Figure 8. Schematic representation of our model for the mechanism of anti-CD63 inhibition. The Lyn–Ca^{2+}-dependent signaling pathway for degranulation is shown in gray. The Ca^{2+}-independent PI3K–Gab2–PKCδ signaling pathway shared with the integrin–tetraspanin complex is shown in black and yellow. Mechanism 1 (steric hindrance of integrin binding to their ECM substrates) is represented in green. Mechanism 2 (general disruption of the membrane complexes containing CD63) is represented in blue. Mechanism 3 (sequestration of PI4K) is represented in red.

comparable Gab2-organized complexes (31) leading to Akt and PKCδ activation (37–41). Adhesion could amplify FcεRI-induced degranulation by increasing the amount of activated Gab2, PI3K, and PKCδ for the FcεRI-induced signaling pathways. This could be accomplished, e.g., if adhesion brought together the plasma membrane microdomains that contain FcεRI with those that contain CD63, its associated integrins and their signaling machinery.

How could anti-CD63 binding to MC exert its inhibitory effect? In CD63 integrin-containing membrane complexes mAb binding to CD63 could either generate an inhibitory signal or block a positive signal for adhesion and FcεRI-induced aggregation. The first possibility would be comparable to the mechanism used by ITIM-containing inhibitory receptors, which upon cross-linking with FcεRI suppress antigen receptor signaling through activation of an inositol phosphatase (18). This seems unlikely since CD63 does not contain an ITIM motif and anti-CD63 did not diminish Ca^{2+} mobilization, which would be observed if an inositol phosphatase such as SHIP was activated by an ITIM (30). Although we cannot exclude that unknown inhibitory signals are activated by anti-CD63, our data provide no support for this hypothesis.

The second possibility (inhibition of a positive signal) is supported by our observation that Gab2 membrane translocation and Akt phosphorylation are suppressed by anti-CD63 in adherent cells even when unstimulated (Fig. 6, A–C). These data suggest that in unstimulated cells, adherence to specific ECM proteins provides a positive signal that can be inhibited by anti-CD63. The inhibition of this positive signal could be generated by at least three different mechanisms (or a combination of them).

First, anti-CD63 could sterically hinder integrin binding to their ECM substrates. This would have a direct effect on adhesion. In this scenario, adhesion would first be inhibited. This steric inhibition would then suppress the adhesion-mediated positive signals involving the Gab2–PI3K pathway with a resulting negative impact on FcεRI-mediated degranulation (Fig. 8, MECHANISM 1).

Second, anti-CD63 could act by generally disrupting the membrane complexes containing CD63, associated integrins and tetraspanins and associated signaling components. This uncoupling of integrins from their signaling molecules would lead to the inhibition of the adhesion-mediated activation of the Gab2–PI3K pathway. Impairment of this pathway would then lead to a decrease in adhesion and subsequently to the inhibition of degranulation (Fig. 8, MECHANISM 2).

Third, anti-CD63 could sequester CD63 and its associated signaling molecules (Fig. 8, MECHANISM 3). Our data on Gab2 and Akt show that anti-CD63 inhibits PIP3 production or an upstream signal. PtdIns-4 kinase (PI4K) associates with CD63 and its sequestration could have such an effect (50). PI4K produces PtdIns-4–P (PI4P), which can be further phosphorylated to PtdIns-4,$5P_2$ (PI4,5P2) by PIP5K. Recently our laboratory has demonstrated the importance of PIP5K in generating PI4,$5P_2$ and in modulating PI3K activation (51). PI4,$5P_2$ is the substrate of PI3Ks. Therefore, local sequestration of PI4K could inhibit specific pools of PI4,$5P_2$ and lead to specific inhibition of selective PI3K isoforms (for example the p110α isoform, see below). This in turn would inhibit the Gab2 pathway and lead to the inhibition of adhesion and degranulation. Note that the PI3K isoform present in the Gab2-organized complex most likely

Downloaded from www.jem.org on February 7, 2005

differs from the one responsible for the membrane targeting of various signaling molecules in the Lyn–Ca^{2+} mobilization pathway, such as Btk or Grb2 (12). Studies showing that antibodies against the p110α isoform of PI3K inhibit degranulation without affecting Ca^{2+} mobilization, whereas antibodies against the p110δ and p110β isoforms inhibit degranulation and Ca^{2+} mobilization (52, 53) suggest that p110α is part of the degranulation pathway, whereas p110δ and p110β are involved in the Lyn–Ca^{2+} mobilization pathway. In summary, we propose that FcεRI-induced degranulation is regulated by adhesion-controlled CD63–integrin membrane complexes whose signaling pathways overlap with those of FcεRI-induced degranulation.

A number of recent studies have demonstrated the efficacy of mAbs as therapeutic tools. Using a rodent model of allergic diseases, we show that anti-CD63 mediated inhibition of MC adhesion and degranulation works in vivo. In the field of allergy, humanized anti-IgE Abs have demonstrated good efficacy and good tolerance. Two recent clinical studies of anti-α4 integrin Ab, one in multiple sclerosis, and one in Crohn's disease (54–56), have shown the therapeutic value and feasibility of interfering with integrin function. Given their capacity to interfere with multiple MC functions, our anti-CD63 mAbs may have therapeutic potential in diseases where MCs are important such as allergic diseases, rheumatoid arthritis, and multiple sclerosis (1, 3).

MATERIALS AND METHODS

Cell culture, reagents, and antibodies. RBL-2H3 and U-937 cells were maintained as described previously (19). Anti-DNP IgE (clone SPE-7) was from Sigma-Aldrich; anti-β1 integrin–CD29 (clone Ha2/5), anti-α5 integrin–CD49e (clone HMα5-1), and anti-β3 integrin–CD61 (clone 2C9.G2) from BD Biosciences; anti-PKCδ (C-17) and anti-Syk (N-19) from Santa Cruz Biotechnology, Inc.; anti-Gab2 from Upstate Biotechnology; anti-phospho–Akt (Ser473) and anti-Akt from Cell Signaling.

Production of mAbs. Hybridomas against RBL were generated as described previously (19). Two hybridomas (7A6 and 12A10) were selected for analysis. Their isotype (IgG1) was determined with a mouse IgG isotyping kit (Amersham Biosciences).

Serotonin release assays. Assays were performed as described in reference 19 with the following modifications. For cells in suspension, the cells were detached after IgE and serotonin loading and incubated with Abs in suspension. Stimulation was performed in BSA-coated tubes under continuous slow rotation. For cells grown on ECM proteins, the cells were attached to ECM protein–coated wells for 16 h as described below for adhesion assays.

LTC4 production. The assay was performed as described in reference 19.

Cloning and expression of rat CD63. Total RNA was isolated from RBL cells using RNAzol B (Tel-Test Inc.) and cDNA was obtained using Omniscript reverse transcriptase (QIAGEN). NH_2-terminal FLAG-tagged CD63 was amplified from the cDNA with Advantage cDNA polymerase (Clontech Laboratories, Inc.) and the following primers: forward 5′-CAGAATTCCCACCATGGGCGACTACAAGGACGACGATGACAAGGCGGTGGAAGGAGGAATGAAGTGTG-3′; reverse 5′-CACAAGCTTGGGCTACATTACTTCGTAGCCACTCC-3′. The 762-bp PCR product was subcloned into the pBJ1neo expression vector. DNA (10 μg) was electroporated in U937 cells (950 μF; 300 V) and selection was initiated 48 h later with 0.6 μg/ml G418 (Invitrogen). Transfected cells were stained with 7A6 and 12A10 and analyzed by flow cytometry.

Immunoblotting and immunoprecipitation. RBL loaded with anti-DNP IgE for 16 h in the presence of 10% FCS under adherent conditions were preincubated with 12A10 or 7A6 (10 μg/ml for 30 min). FcεRI aggregation was performed as for serotonin release assays. For analysis of PKCδ activity under nonadherent conditions, cells were detached using 0.05% trypsin after loading with IgE. Preincubation with 12A10 and FcεRI aggregation were performed in polypropylene tubes under continuous slow rotation. Cells were lyzed and lysates were blotted and precipitated according to standard procedures. For separation of membrane and cytosolic fractions cells were scraped in homogenization buffer (25 mM Hepes, pH 7.4, 5 mM EGTA, 50 mM NaF, and a protease inhibitor cocktail). After homogenization in a Dounce homogenizer, cell debris was removed by centrifugation (800 *g* for 5 min at 4°C) and the supernatant was centrifuged to pellet membranes (250,000 *g* for 30 min at 4°C). The pellet was resuspended in 200 μl homogenization buffer and analyzed by SDS-PAGE and Western blotting as in reference 57.

Adhesion assays. 96-well tissue culture plates were coated with 10 μg/ml fibronectin, vitronectin, or fibrinogen (all Sigma-Aldrich) in PBS for 16 h at room temperature and blocked with 2% BSA in Ca^{2+}/Mg^{2+}-free PBS for 2 h at 37°C. RBL were starved in culture medium without FCS for 16 h. They were then detached and incubated in Eagle's minimal essential medium containing 0.1% BSA (without FCS) with Abs at 10–40 μg/ml for 1 h at 37°C. After washing the cells were incubated in the coated wells for 30 min at 37°C. They were then washed and fixed with 2.5% formaldehyde. After washing with PBS, staining was performed for 1 h at room temperature with 0.1% crystal violet and the cells were lysed in 10% acetic acid. Adhesion was quantified by reading absorption of the incorporated dye at 570 nm.

Ca^{2+} measurements. RBL were seeded onto 10 mm glass coverslips at 0.4×10^6/ml in culture medium with 0.2 μg/ml anti-DNP IgE for 16 h. Cells were then loaded with fura-2 a.m. ester as described in reference 26 and with 10 μg/ml Ab for 45 min at 37°C. The coverslips were placed into a holding device inside the cuvette of a Deltascan spectrofluorometer (PTI) and analysis was performed as described previously (24). 340:380 ratios (R) were normalized to the average baseline ratios during the first 60 s of recording (R_0). The area under the curve for each experiment was calculated and an unpaired *t* test was performed using Prism4 software (GraphPad Software).

PKCδ kinase assays. For assessment of PKCδ kinase activity, anti-PKCδ immunoprecipitates from 5×10^6 RBL-2H3 cells were incubated in 20 μl kinase buffer (57) plus 10 μl substrate mix containing 1 μg MBP (Sigma-Aldrich), 50 μM ATP, and 10 μCi [γ^{32}P]-ATP (NEN Life Science Products) for 30 min at room temperature. Reactions were stopped with one volume of 2× SDS sample buffer and samples were separated by SDS-PAGE. Analysis of phosphorylated bands was performed on a Molecular Imager (Bio-Rad Laboratories). Immunoprecipitates were analyzed for equal amounts of the PKCδ using immunoblots with anti-PKCδ antibodies.

Passive cutaneous anaphylaxis (PCA). PCA assays were performed as described previously (19).

Statistical analysis. Statistical analysis was performed with the Mann-Whitney test for ungrouped variables and the Wilcoxon test for grouped variables using StatView 5.0.1 software (SAS Institute Inc.).

We thank Dr. R. Siraganian (Receptors and Signal Transduction Section, National Institutes of Health [NIH], Bethesda, MD) for providing the anti-CD63 mAb AD1.

S. Kraft was supported in part by an Emmy Noether Fellowship from Deutsche Forschungsgemeinschaft. This work was supported by an NIH grant (AI46734-01). Beth Israel Deaconess Medical Center has filed a US patent application based on the data presented here.

The authors have no conflicting financial interests.

Downloaded from www.jem.org on February 7, 2005

Submitted: 11 October 2004
Accepted: 16 November 2004

REFERENCES

1. Benoist, C., and D. Mathis. 2002. Mast cells in autoimmune disease. *Nature*. 420:875–878.
2. Galli, S.J., M. Maurer, and C.S. Lantz. 1999. Mast cells as sentinels of innate immunity. *Curr. Opin. Immunol.* 11:53–59.
3. Williams, C.M., and S.J. Galli. 2000. The diverse potential effector and immunoregulatory roles of mast cells in allergic disease. *J. Allergy Clin. Immunol.* 105:847–859.
4. Kinet, J.P. 1999. The high-affinity IgE receptor (FcεRI): from physiology to pathology. *Annu. Rev. Immunol.* 17:931–972.
5. Columbo, M., B.S. Bochner, and G. Marone. 1995. Human skin mast cells express functional β1 integrins that mediate adhesion to extracellular matrix proteins. *J. Immunol.* 154:6058–6064.
6. Columbo, M., and B.S. Bochner. 2001. Human skin mast cells adhere to vitronectin via the αvβ3 integrin receptor (CD51/CD61). *J. Allergy Clin. Immunol.* 107:554.
7. Thompson, H.L., P.D. Burbelo, and D.D. Metcalfe. 1990. Regulation of adhesion of mouse bone marrow-derived mast cells to laminin. *J. Immunol.* 145:3425–3431.
8. Dastych, J., and D.D. Metcalfe. 1994. Stem cell factor induces mast cell adhesion to fibronectin. *J. Immunol.* 152:213–219.
9. Apgar, J.R. 1997. Increased degranulation and phospholipase A2, C, and D activity in RBL cells stimulated through FcεR1 is due to spreading and not simply adhesion. *J. Cell Sci.* 110:771–780.
10. Hamawy, M.M., C. Oliver, S.E. Mergenhagen, and R.P. Siraganian. 1992. Adherence of rat basophilic leukemia (RBL-2H3) cells to fibronectin-coated surfaces enhances secretion. *J. Immunol.* 149:615–621.
11. Yasuda, M., Y. Hasunuma, H. Adachi, C. Sekine, T. Sakanishi, H. Hashimoto, C. Ra, H. Yagita, and K. Okumura. 1995. Expression and function of fibronectin binding integrins on rat mast cells. *Int. Immunol.* 7:251–258.
12. Turner, H., and J.P. Kinet. 1999. Signalling through the high-affinity IgE receptor FcεRI. *Nature*. 402:B24–B30.
13. Hirasawa, N., F. Santini, and M.A. Beaven. 1995. Activation of the mitogen-activated protein kinase/cytosolic phospholipase A2 pathway in a rat mast cell line. Indications of different pathways for release of arachidonic acid and secretory granules. *J. Immunol.* 154:5391–5402.
14. Hirasawa, N., A. Scharenberg, H. Yamamura, M.A. Beaven, and J.P. Kinet. 1995. A requirement for Syk in the activation of the microtubule-associated protein kinase/phospholipase A2 pathway by FcεR1 is not shared by a G protein-coupled receptor. *J. Biol. Chem.* 270:10960–10967.
15. Zhang, C., N. Hirasawa, and M.A. Beaven. 1997. Antigen activation of mitogen-activated protein kinase in mast cells through protein kinase C-dependent and independent pathways. *J. Immunol.* 158:4968–4975.
16. Parravicini, V., M. Gadina, M. Kovarova, S. Odom, C. Gonzalez-Espinosa, Y. Furumoto, S. Saitoh, L.E. Samelson, J.J. O'Shea, and J. Rivera. 2002. Fyn kinase initiates complementary signals required for IgE-dependent mast cell degranulation. *Nat. Immunol.* 3:741–748.
17. Gu, H., K. Saito, L.D. Klaman, J. Shen, T. Fleming, Y. Wang, J.C. Pratt, G. Lin, B. Lim, J.P. Kinet, and B.G. Neel. 2001. Essential role for Gab2 in the allergic response. *Nature*. 412:186–190.
18. Katz, H.R. 2002. Inhibitory receptors and allergy. *Curr. Opin. Immunol.* 14:698–704.
19. Fleming, T.J., E. Donnadieu, C.H. Song, F.V. Laethem, S.J. Galli, and J.P. Kinet. 1997. Negative regulation of FcεRI-mediated degranulation by CD81. *J. Exp. Med.* 186:1307–1314.
20. Kitani, S., E. Berenstein, S. Mergenhagen, P. Tempst, and R.P. Siraganian. 1991. A cell surface glycoprotein of rat basophilic leukemia cells close to the high affinity IgE receptor (FcεRI). Similarity to human melanoma differentiation antigen ME491. *J. Biol. Chem.* 266:1903–1909.
21. Nishikata, H., C. Oliver, S.E. Mergenhagen, and R.P. Siraganian. 1992. The rat mast cell antigen AD1 (homologue to human CD63 or melanoma antigen ME491) is expressed in other cells in culture. *J. Immunol.* 149:862–870.
22. Boucheix, C., and E. Rubinstein. 2001. Tetraspanins. *Cell. Mol. Life Sci.* 58:1189–1205.
23. Hemler, M.E. 2001. Specific tetraspanin functions. *J. Cell Biol.* 155: 1103–1107.
24. Zhang, X.A., A.L. Bontrager, and M.E. Hemler. 2001. Transmembrane-4 superfamily proteins associate with activated protein kinase C (PKC) and link PKC to specific β1 integrins. *J. Biol. Chem.* 276: 25005–25013.
25. Mannion, B.A., F. Berditchevski, S.K. Kraeft, L.B. Chen, and M.E. Hemler. 1996. Transmembrane-4 superfamily proteins CD81 (TAPA-1), CD82, CD63, and CD53 specifically associated with integrin α4 β1 (CD49d/CD29). *J. Immunol.* 157:2039–2047.
26. Berditchevski, F., G. Bazzoni, and M.E. Hemler. 1995. Specific association of CD63 with the VLA-3 and VLA-6 integrins. *J. Biol. Chem.* 270:17784–17790.
27. Radford, K.J., R.F. Thorne, and P. Hersey. 1997. Regulation of tumor cell motility and migration by CD63 in a human melanoma cell line. *J. Immunol.* 158:3353–3358.
28. Ozawa, K., Z. Szallasi, M.G. Kazanietz, P.M. Blumberg, H. Mischak, J.F. Mushinski, and M.A. Beaven. 1993. Ca2+-dependent and Ca2+-independent isozymes of protein kinase C mediate exocytosis in antigen-stimulated rat basophilic RBL-2H3 cells. Reconstitution of secretory responses with Ca2+ and purified isozymes in washed permeabilized cells. *J. Biol. Chem.* 268:1749–1756.
29. Nishizumi, H., and T. Yamamoto. 1997. Impaired tyrosine phosphorylation and Ca2+ mobilization, but not degranulation, in lyn-deficient bone marrow-derived mast cells. *J. Immunol.* 158:2350–2355.
30. Scharenberg, A.M., O. El-Hillal, D.A. Fruman, L.O. Beitz, Z. Li, S. Lin, I. Gout, L.C. Cantley, D.J. Rawlings, and J.P. Kinet. 1998. Phosphatidylinositol-3,4,5-trisphosphate (PtdIns-3,4,5-P3)/Tec kinase-dependent calcium signaling pathway: a target for SHIP-mediated inhibitory signals. *EMBO J.* 17:1961–1972.
31. Yu, W.M., T.S. Hawley, R.G. Hawley, and C.K. Qu. 2002. Role of the docking protein Gab2 in β1-integrin signaling pathway-mediated hematopoietic cell adhesion and migration. *Blood.* 99:2351–2359.
32. Xie, Z.H., I. Ambudkar, and R.P. Siraganian. 2002. The adapter molecule Gab2 regulates FcεRI-mediated signal transduction in mast cells. *J. Immunol.* 168:4682–4691.
33. Kitaura, J., K. Asai, M. Maeda-Yamamoto, Y. Kawakami, U. Kikkawa, and T. Kawakami. 2000. Akt-dependent cytokine production in mast cells. *J. Exp. Med.* 192:729–740.
34. Stephens, L., K. Anderson, D. Stokoe, H. Erdjument-Bromage, G.F. Painter, A.B. Holmes, P.R. Gaffney, C.B. Reese, F. McCormick, P. Tempst, et al. 1998. Protein kinase B kinases that mediate phosphatidylinositol 3,4,5-trisphosphate-dependent activation of protein kinase B. *Science*. 279:710–714.
35. Franke, T.F., S.I. Yang, T.O. Chan, K. Datta, A. Kazlauskas, D.K. Morrison, D.R. Kaplan, and P.N. Tsichlis. 1995. The protein kinase encoded by the Akt proto-oncogene is a target of the PDGF-activated phosphatidylinositol 3-kinase. *Cell.* 81:727–736.
36. Gu, H., R.J. Botelho, M. Yu, S. Grinstein, and B.G. Neel. 2003. Critical role for scaffolding adapter Gab2 in FcγR-mediated phagocytosis. *J. Cell Biol.* 161:1151–1161.
37. Fornaro, M., J. Plescia, S. Chheang, G. Tallini, Y.M. Zhu, M. King, D.C. Altieri, and L.R. Languino. 2003. Fibronectin protects prostate cancer cells from TNFα-induced apoptosis via the AKT/survivin pathway. *J. Biol. Chem.* 278:50402–50411.
38. Matter, M.L., and E. Ruoslahti. 2001. A signaling pathway from the α5β1 and αvβ3 integrins that elevates bcl-2 transcription. *J. Biol. Chem.* 276:27757–27763.
39. Roberts, M.S., A.J. Woods, T.C. Dale, P. Van Der Sluijs, and J.C. Norman. 2004. Protein kinase B/Akt acts via glycogen synthase kinase 3 to regulate recycling of αvβ3 and α5β1 integrins. *Mol. Cell. Biol.* 24: 1505–1515.
40. Zheng, D.Q., A.S. Woodard, G. Tallini, and L.R. Languino. 2000. Substrate specificity of αvβ3 integrin-mediated cell migration and PI3-kinase/AKT pathway activation. *J. Biol. Chem.* 275:24565–24574.
41. Lam, K., L. Zhang, K.M. Yamada, and R.M. Lafrenie. 2001. Adhesion of epithelial cells to fibronectin or collagen I induces alterations in gene

Downloaded from www.jem.org on February 7, 2005

expression via a protein kinase C-dependent mechanism. *J. Cell. Physiol.* 189:79–90.
42. Chang, E.Y., Z. Szallasi, P. Acs, V. Raizada, P.C. Wolfe, C. Fewtrell, P.M. Blumberg, and J. Rivera. 1997. Functional effects of overexpression of protein kinase C-α, -β, -δ, -ε, and -η in the mast cell line RBL-2H3. *J. Immunol.* 159:2624–2632.
43. Razin, E., Z. Szallasi, M.G. Kazanietz, P.M. Blumberg, and J. Rivera. 1994. Protein kinases C-β and C-ε link the mast cell high-affinity receptor for IgE to the expression of c-fos and c-jun. *Proc. Natl. Acad. Sci. USA.* 91:7722–7726.
44. Berditchevski, F. 2001. Complexes of tetraspanins with integrins: more than meets the eye. *J. Cell Sci.* 114:4143–4151.
45. Feigelson, S.W., V. Grabovsky, R. Shamri, S. Levy, and R. Alon. 2003. The CD81 tetraspanin facilitates instantaneous leukocyte VLA-4 adhesion strengthening to VCAM-1 under shear flow T. *J. Biol. Chem.* 278:51203–51212.
46. Vial, D., H. Okazaki, and R.P. Siraganian. 2000. The NH2-terminal region of focal adhesion kinase reconstitutes high affinity IgE receptor-induced secretion in mast cells. *J. Biol. Chem.* 275:28269–28275.
47. Hamawy, M.M., S.E. Mergenhagen, and R.P. Siraganian. 1993. Tyrosine phosphorylation of pp125FAK by the aggregation of high affinity immunoglobulin E receptors requires cell adherence. *J. Biol. Chem.* 268:6851–6854.
48. Vial, D., C. Oliver, M.C. Jamur, M.V. Pastor, E. da Silva Trindade, E. Berenstein, J. Zhang, and R.P. Siraganian. 2003. Alterations in granule matrix and cell surface of focal adhesion kinase-deficient mast cells. *J. Immunol.* 171:6178–6186.
49. Geng, L., S. Pfister, S.K. Kraeft, and C.E. Rudd. 2001. Adaptor FYB (Fyn-binding protein) regulates integrin-mediated adhesion and mediator release: differential involvement of the FYB SH3 domain. *Proc. Natl. Acad. Sci. USA.* 98:11527–11532.
50. Berditchevski, F., K.F. Tolias, K. Wong, C.L. Carpenter, and M.E. Hemler. 1997. A novel link between integrins, transmembrane-4 superfamily proteins (CD63 and CD81), and phosphatidylinositol 4-kinase. *J. Biol. Chem.* 272:2595–2598.
51. Saito, K., K.F. Tolias, A. Saci, H.B. Koon, L.A. Humphries, A. Scharenberg, D.J. Rawlings, J.P. Kinet, and C.L. Carpenter. 2003. BTK regulates PtdIns-4,5-P2 synthesis: importance for calcium signaling and PI3K activity. *Immunity.* 19:669–678.
52. Smith, A.J., Z. Surviladze, E.A. Gaudet, J.M. Backer, C.A. Mitchell, and B.S. Wilson. 2001. p110β and p110δ phosphatidylinositol 3-kinases up-regulate FcεRI-activated Ca2+ influx by enhancing inositol 1,4,5-trisphosphate production. *J. Biol. Chem.* 276:17213–17220.
53. Windmiller, D.A., and J.M. Backer. 2003. Distinct phosphoinositide 3-kinases mediate mast cell degranulation in response to G-protein-coupled versus FcεRI receptors. *J. Biol. Chem.* 278:11874–11878.
54. Miller, D.H., O.A. Khan, W.A. Sheremata, L.D. Blumhardt, G.P. Rice, M.A. Libonati, A.J. Willmer-Hulme, C.M. Dalton, K.A. Miszkiel, and P.W. O'Connor. 2003. A controlled trial of natalizumab for relapsing multiple sclerosis. *N. Engl. J. Med.* 348:15–23.
55. Ghosh, S., E. Goldin, F.H. Gordon, H.A. Malchow, J. Rask-Madsen, P. Rutgeerts, P. Vyhnalek, Z. Zadorova, T. Palmer, and S. Donoghue. 2003. Natalizumab for active Crohn's disease. *N. Engl. J. Med.* 348:24–32.
56. von Andrian, U.H., and B. Engelhardt. 2003. α4 Integrins as therapeutic targets in autoimmune disease. *N. Engl. J. Med.* 348:68–72.
57. Storz, P., and A. Toker. 2003. Protein kinase D mediates a stress-induced NF-κB activation and survival pathway. *EMBO J.* 22:109–120.

Downloaded from www.jem.org on February 7, 2005